Mixed systems based on aminated and sulfonated silica nanoparticles: synthesis, self-assembly, and selective adsorption of certain biopolymers*

L. S. Yakimova,[a] A. R. Nugmanova,[a] V. G. Evtugyn,[b] Yu. N. Osin,[b] and I. I. Stoikov[a]★

[a]*Kazan Federal University, A. M. Butlerov Chemical Institute, 18 ul. Kremlevskaya, 420008 Kazan, Russian Federation. E-mail: ivan.stoikov@mail.ru*
[b]*Kazan Federal University, Interdisciplinary Center Analytical Microscopy, 18 ul. Kremlevskaya, 420008 Kazan, Russian Federation*

Hybrid aminated and sulfonated nanoparticles were synthesized by surface modification of silica nanopowder with 3-aminopropyltriethoxysilane and 1,3-propanesultone, respectively. The developed protocols for the synthesis of three types of "buffer" mixed submicron particles with corresponding ζ-potentials (−21.4±1.3, 4.7±0.4, 12.4±0.8) were based on various methods of nanoprecipitation of synthesized silica nanoparticles modified by amino- and sulfonate groups, and on various conditions of these precepitation (solvent, temperature). Hybrid SiO_2 particles, as well as self-assembling associates based on sulfonated and aminated particles, were examined in extraction of biologically important macromolecules. It was established that the efficiency of adsorption of calf thymus DNA increased with increasing zeta potentials of the modified silica particles studied. The interaction of the studied model proteins (bovine serum albumin and lysozyme) with the synthesized silica nanoparticles modified by sulfonate groups increased as the pH of the medium decreased.

Key words: silica, surface modification, self-assembly, self-organization, calf thymus DNA, bovine serum albumin, lyzozyme.

In recent years, much attention has been paid to silica nanoparticles since they are applied as a basic component in developing hybrid organic-inorganic materials[1—4] owing to the specific properties of silica[5] and nanoparticles.[6] Organosilicon hybrid materials have gained vogue due to their unique, practical physicochemical characteristics. They are used as sorbents,[7] catalysts,[8] chromatographic stationary phases,[9] for the development of sensors,[10] *etc*. Nanostructures of silica modified by various organosilicon precursors are widely utilized in biomedicine. Development and implementation of such nanoparticles for biomedical applications is primarily due to their low toxicity,[11] biocompatibility,[11] as well as an ability to control the size and shape of synthesized nanostructures.[12,13] Organosilicon hybrid materials are used as high-quality contrasting agents[14] in biomedical imaging and analysis,[15] as well as targeted drug delivery agent.[11] Investigation of the interaction of macromolecules with surfaces of highly dispersed solid materials is necessary for the development of technological processes in biochemistry and medicine in addition to that it is relevant for a better understanding the fundamental aspects of adsorption. Currently, much attention is paid to fundamental research on the interaction of macromolecules with silica nanoparticles as carriers for drug immobilization.[16]

A number of studies have shown that the nature organosilicon modifiers covalently linked on the surface of silica is responsible both for the chemical properties of surface-modified materials[1—4] and for the adsorption characteristics of biologically important macromolecules.[17—19] The usage of modifiers which are able to chemically react with the surface silanol groups makes it possible to control and reproduce the formation of the anchored layer during the synthesis of SiO_2 nanoparticles and/or during the subsequent treatment of silica.[20]

In this paper, we studied self-assembly and self-organization of mixed particles based on two types of silica nanoparticles: functionalized by amino and sulfonate groups. In addition, the sorption capacity of these particles in respect to biopolymers (calf thymus DNA, bovine serum albumin and lysozyme) was determined.

Experimental

^{1}H NMR spectra were recorded on a BrukerAvance-400 spectrometer (400 MHz) in D_2O, and IR spectra were recorded on a Spectrum 400 Fourier spectrometer (Perkin—Elmer). The

* Dedicated to Academician of the Russian Academy of Sciences A. I. Konovalov on the occasion of his 85th birthday.

Published in Russian in *Izvestiya Akademii Nauk. Seriya Khimicheskaya,* No. 2, pp. 0262—0269, February, 2019.
1066-5285/19/6802-0262

particle size in the solution was determined by dynamic light scattering (DLS) on a Zetasizer Nano ZS (Malvern) nanoparticle size analyzer equipped with a He—Ne laser (4 mV; wavelength of 633 nm); the angle of detection of scattered light was 173°, measurement positions inside the cuvette were determined automatically. Electron absorption spectra were recorded on a Shimadzu UV-3600 spectrometer, with the transmissive layer thickness of 1 cm. Samples were sonicated using a Sonics Vibracell VCX 500 instrument using a step microtype (3 mm in diameter) immersed in a mixture of solvent and undissolved substance. The simultaneous thermogravimetry and differential scanning calorimetry (TG/DSC) analysis was carried out on a STA 449 C Jupiter (Netzsch) thermal analyzer in 40 μL platinum crucibles with a pierced lid (0.5 mm in diameter). The measurements were performed at constant heating rates (10 and 4 K min^{-1}) in a dynamic argon atmosphere at a flow rate of 20 mL min^{-1} and atmospheric pressure. Samples weighing 10—20 mg were used for analyses. The heating range was 303—1173 K. Transmission electron microscopy (TEM) images were obtained on a JEOL JEM 100CXII microscope. The samples were prepared on a nickel grid (150 Mesh) covered with formvar by evaporation of aqueous or methanol solutions (concentration of 10^{-4} g mL^{-1}) for 1 h. Deionized water of the first stage of purification (with a resistance of >18.0 MΩ cm at 25 °C) was obtained from distilled water using Millipore-Q system.

Surface modification of silica nanoparticles with 3-aminopropyltriethoxysilane. Silica nanopowder (Sigma—Aldrich, 12 nm, surface area 175–225 m^2 g^{-1} (BET), 0.3 g, 5 mmol) was dispersed in 15 mL of methanol at ultrasonic treatment for 1 h. A solution of 0.12 mL (0.5 mmol) of 3-aminopropyltriethoxysilane (APTES) in 15 mL of methanol was added dropwise to the colloidal suspension. After ultrasonic treatment for 60 min, the colloidal solution was kept for 24 h to condense the organosilicon modifier on the surface of the nanoparticles. Then the colloidal suspension was washed with methanol (3×30 mL): 30 mL of methanol was added to the reaction mixture, stirred, and centrifuged. After centrifugation, the dispersed phase and the dispersion medium were separated (methanol, polycondensation products), the latter was removed by decantation. The procedure was repeated three times. The yield of particle **I** was 0.28 g (95%).

IR, ν/cm^{-1}: 1651 (H—O linked water); 1490 (Si—O—H—NH_2^+); 972 (CH_2); 1190, 1112, 799, 721, 474 (Si—O—Si). ^{1}H NMR (D_2O), δ: 0.69 (m, 2 H, $SiCH_2$); 1.76 (m, 2 H, CH_2); 3.00 (m, 2 H, CH_2NH_2).

Surface modification of silica nanoparticles with 1,3-propanesultone. Silica nanopowder (0.3 g, 5 mmol) was dispersed in 15 mL of toluene by ultrasonic treatment for 1 h. A mixture containing 0.06 g (0.5 mmol) of 1,3-propansultone in 15 mL of toluene was added dropwise to the colloidal suspension. After ultrasonic treatment for 60 min, the mixture was heated for 48 h at the boiling point of toluene. Then the colloidal suspension was washed with methanol (3×30 mL): 30 mL of methanol was added to the reaction mixture, stirred, and centrifuged. After centrifugation, the dispersed phase and the dispersion medium were separated (methanol, 1,3-propanesultone, polycondensation products), the latter was removed by decantation. The procedure was repeated three times. The yield of particle **II** was 0.28 g (95%).

IR, ν/cm^{-1}: 1440—1480, 1586, 2970—3057 (CH_2); 1068—1101 (Si—O—Si); 814 (Si—OH); 738, 1379 (SO_3H). ^{1}H NMR (D_2O), δ: 1.15 (m, 2 H, $SiCH_2$); 1.94 (m, 2 H, CH_2); 2.97 (m, 2 H, CH_2SO_3H).

Calculation of amount of functional groups per 1 m^2 of surface of synthesized materials. Commercial silica was characterized by the surface area of 175—225 m^2 g^{-1} (BET). The amount of 3-aminopropyltriethoxysilane and 1,3-propanesultone used to modify the silica particles was 0.11 g ($5\cdot10^{-4}$ mol) and 0.31 g ($2.5\cdot10^{-3}$ mol), respectively. Taking into account the surface area (S, m^2) and the amount of modifier (the number of moles of the modifier ν, mol) and using the formula $n = \nu/(Sm)$, where m is the weight of the modifier (g), we found that the number of functional groups per 1 m^2 (n) was 0.020—0.026 ($5\cdot10^{-4}/(225\cdot0.11)$ and $5\cdot10^{-4}/(175\cdot0.11)$) and 0.036—0.046 ($2.5\cdot10^{-3}/(225\cdot0.31)$ and $2.5\cdot10^{-3}/(175\cdot0.31)$) mmol per 1 m^2 for aminated and sulphonated particles, respectively.

Mixed particle syntheses. *Mixed particles* **III.** (1) Sulfonated particles **II** were produced from 0.3 g (5 mmol) of silica nanoparticles and 2.5 mmol of 1,3-propanesultone; aminated particles **I** were produced from 0.3 g (5 mmol) of silica nanoparticles and 0.5 mmol of APTES; (2) after modifying the surface of silica nanoparticles, the hybrid particles were centrifuged in toluene or methanol for sulfonated and aminated particles, respectively; (3) to obtain powders of isolated aminated and sulfonated particles, the solvents were evaporated under reduced pressure. The solutions of sulfonated (**II**) and aminated (**I**) SiO_2 nanoparticles, which were obtained by ultrasonic dispersion of powders in water, were mixed in an equivalent amount to produce mixed particles **III**.

Mixed particles **IV** *and* **V.** This method for the mixed particle formation consisted in mixing solutions of as-synthesized particles **I** and **II**. For these syntheses, 0.3 g (5 mmol) of silica nanoparticles and the same amount of 1,3-propanesultone and APTES (0.5 mmol) were used. After colloidal solutions of aminated and sulfonated silica nanoparticles were obtained, they were mixed in equal quantities. As soon as formation of hybrid associates (by using the second method) completed, the particles were isolated from ethanol, low-molecular compounds, as well as from a mixture of solvents (toluene and methanol) by three times repeated centrifugation cycle in acetone. After removal of acetone at ~20 °C, a white powder (**IV**) remained, part of which was subjected to heat treatment at 220 °C (**V**). Thus, three types of hybrid particles were obtained from sulfonated and aminated silica particles.

Efficiency of the adsorbate extraction from the solution. The sorbent and sorbate were used in a ratio of 1 : 1. Buffer solutions of particles and biopolymers (calf thymus DNA, bovine serum albumin, lysozyme) were stirred with equal concentration for 3 h at ~20 °C, and then the aqueous solution which was above the sorbent layer was separated using a nylon filter (0.45 μm). The residual concentration of the solute in the filtrate was measured using a UV spectrometer (the absorption maximum was determined for each adsorbate: DNA or protein).

The time for sorbent saturation was determined by studying the sorption kinetics at stirring the sorbate—sorbent systems on a magnetic stirrer at 25±2 °C. After sorption, specified amounts of solutions were sampled at different time (0.5, 1, 2, and 3 h), filtered (0.45 μm), and electron absorption spectra were recorded for these aqueous solutions. It was found that after 3 h, the optical density of the analyzed solutions did not change, and this corresponds to the maximum saturation of the sorbent.

The efficiency of the adsorbate extraction from the solution R (%) was calculated using Eq. (1):

$$R = (c_0 - c_a)/c_0 \cdot 100\%, \quad (1)$$

where c_0 and c_a (mg L^{-1}) are the initial and residue concentrations of adsorbate, respectively.

As $A \sim c$ according to the Bouguer— Lambert—Beer law, we can write Eq. (2):

$$R = (A_0 - A_a)/A_0 \cdot 100\%, \quad (2)$$

where A_0 and A_a are the optical density of the solution before and after the sorption, respectively. Each adsorption experiment was repeated 3 times, and the average values are shown in the experimental results.

Determination of association constants $\log K_{ass}$ using spectroscopy in the visible and UV regions. To registrate UV spectra, 100 μL of the solution of particles **II** ($2.0 \cdot 10^{-5}$ g mL^{-1}) were added to 100, 200, 300, 400, 500, 600, 700, 800, 900, or 1000 μL of $1.6 \cdot 10^{-5}$ *M* solution of BSA in buffer and adjusted to a volume of 3 mL using buffer.

The balance of the system is described by Eq. (3):

$$n\,G + H \rightleftharpoons G_nH, \quad (3)$$

where H, G, and G_nH correspond to the ligand (particles **II**), the substrate (BSA) and the complex with the substrate, respectively, n is the number of substrates which react with one ligand.

The association constant was found using Eq. (4):

$$K_{ass} = [G_nH]/([G]^n[H]). \quad (4)$$

To determine the stoichiometric coefficient *n* of the complex, Eq. (4) was transformed into Eq. (5):

$$\log K_{ass} = \log[G_nH] - n\log[G] - \log[H]. \quad (5)$$

In a UV spectrum, the absorbance *A*, which corresponds to the maximum absorption band at a certain wavelength, is the sum of the absorption values of the components. It can be expressed by Eq. (6):

$$A = A_{G_nH} + A_H, \quad (6)$$

where A_{G_nH} and A_H are absorption values for the complex and ligand, respectively.

Since the Bouguer— Lambert—Beer law is correct for all components of the solution, Eq. (7) can be derived:

$$A_i = C_i \varepsilon_i l, \quad (7)$$

where A_i is the absorption of the *i*th component of the solution, C_i is its molar concentration, E_i is its extinction coefficient, *l* is the length of the absorbing layer. The concentration of the complex $[G_nH]$ in the system was calculated according to Eqs (6) and (7).

The plot of $\log[G_nH] - \log[H]$ versus $\log[G]$ (see below) is a line, the slope of which corresponds to n. The association constant was calculated taking into account the cross point with the axis of ordinates (8):

$$b = \log K_{ass}. \quad (8)$$

To determine the association constant for each system, three independent experiments were carried out. Statistical data processing was performed using Student′s *t*-test.

Results and Discussion

Synthesis of aminated and sulfonated nanoparticles of sillica. The presence of surface functional groups which govern the surface charge, the length of alkyl groups of the linkers between charged fragments and carrier, as well as structural characteristics of material have impact on the efficiency of interaction and adsorption of biologically important macromolecules on hybrid silica particles. To anchor DNA and various protein molecules, polyfunctional fragments of surface-modified SiO_2 which contain sulfonate and amino groups are considered as promising agents. This is due to the simplicity of functionalization of silica nanoparticle with corresponding modifier, low toxicity of silica, and relatively low prices of reagents.

Surface modification of silica nanopowder (particles of 12 nm) was performed by immobilizing organosilicon modifiers in order to obtain both positively and negatively charged nanoparticles. APTES was used to obtain positively charged SiO_2 nanoparticles (**I**), and 1,3-propansultone was used for negatively charged ones (**II**) (Scheme 1). Functionalization of SiO_2 nanoparticles was confirmed by ^{1}H NMR spectroscopy, UV, and IR spectroscopy.

Scheme 1

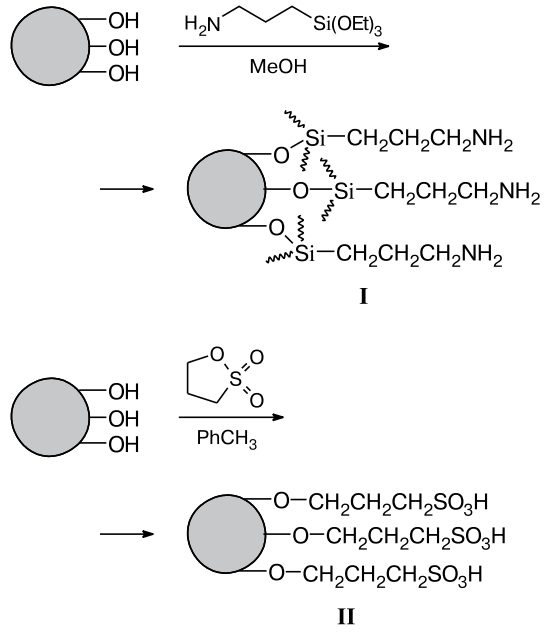

In the ^{1}H NMR spectrum of aminated nanoparticles **I** dispersed in water, a multiplet in the δ 0.69 region corresponded to the methylene group protons ($SiCH_2$) bound to silicon; a multiplet peak in δ 3.00 region corresponded to the methylene group protons (CH_2NH) bound to the amino group; and a multiplet signal in the δ 1.76 range was attributed to the protons of the methylene group in $CH_2C\underline{H}_2CH_2$ fragment (Fig. 1).

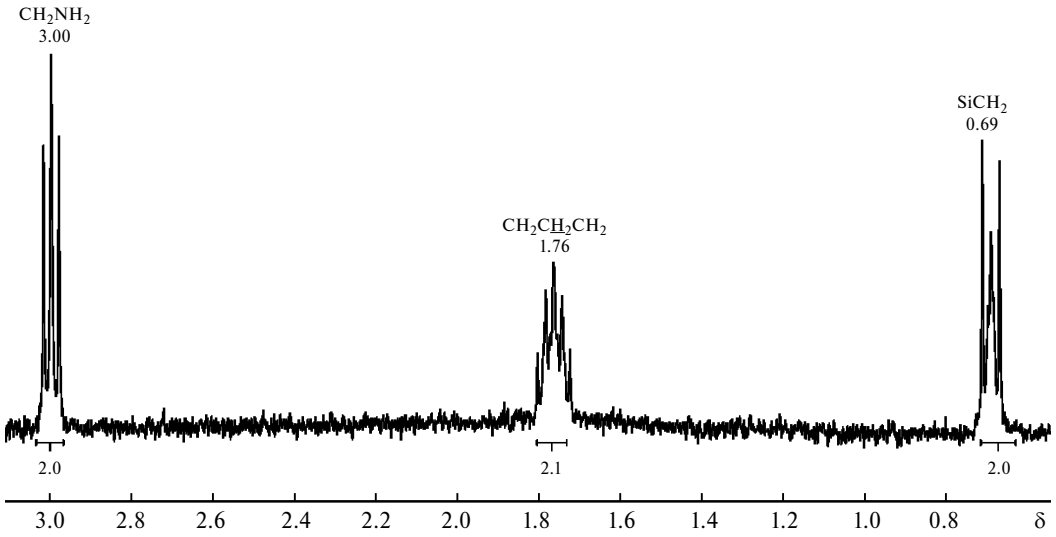

Fig. 1. ^{1}H NMR spectra of aminated nanoparticled SiO_2 **(I)** (D_2O, 25 °C, Bruker Avance-400).

The temperature dependence of the rate of weight loss of silica nanoparticles **I** and **II** was registrated by a combined TG/DSC method. The total weight loss was 3—9% which is an evidence of that the reaction of silica nanopowder with the corresponding organic surface modifier (Fig. 2) occured. As it follows from the analysis, decomposition of aminated and sulfonated SiO_2 nanoparticles proceeded in several stages: firstly, water molecules evolved (0.95 and 1.84 wt.%, respectively), and the following stages — second, third, and fourth stages — corresponded to decomposition of organic fragments chemically adsorbed on silica surface (1.10, 4.66 and 2.61 wt.% for the aminated SiO_2 particles; 1.84, 2.21 and 0.84 wt.% for the sulfonated SiO_2 particles).

The amount of organic substituents on the surface of silica particles, estimated by TG/DSC, was 0.036—0.046 and 0.020—0.026 mmol m^{-2} for aminated and sulfonated particles, respectively.

Dimensions of associates forming surface-modified particles **I** and **II** were estimated by DLS. In the case of aminated nanoparticles **I**, those were colloidal systems with a polydispersity index of 0.09 and associates with a diameter of 186 nm. Sulfonated particles **II** represented as monodisperse systems with a polydispersity index of 0.23 and associates with a diameter of 201 nm. The sizes of nanoparticles **I** and **II**, of which the corresponding associates consisted, were measured by TEM, and estimated as 18 and 23 nm, respectively (Fig. 3). Using TEM technique, it was shown that spherical particles were produced as a result of silica nanopowder functionalization by organic (organiosilicon) surface modifiers (see Fig. 3).

The stability of colloidal systems was studied by DLS. Based on the values of ζ-potentials of aqueous solutions of aminated and sulfonated silica particles, we could conclude about satisfying stability of sulfonated silica suspensions, which ζ-potential was −43.1, and about lower stability of aminated particles, which ζ-potential was +11.3.

Self-assembly and self-organization of particles based on aminated and sulfonated hybrid silica nanoparticles I and II were applied to synthesize mixed particles **III**, **IV** and **V**. Self-assembly was conducted using two approaches. In the first one, two solutions of sulfonated and aminated SiO_2 nanoparticles, obtained by ultrasonic dispersion of

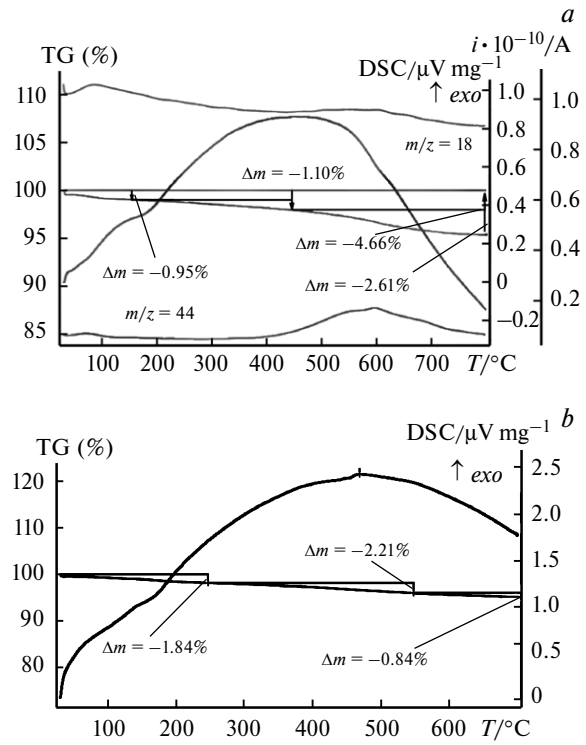

Fig. 2. TG/DSC data of aminated nanoparticled SiO_2 **(I)** (*a*) and sulfonated nanoparticles SiO_2 **(II)** (*b*).

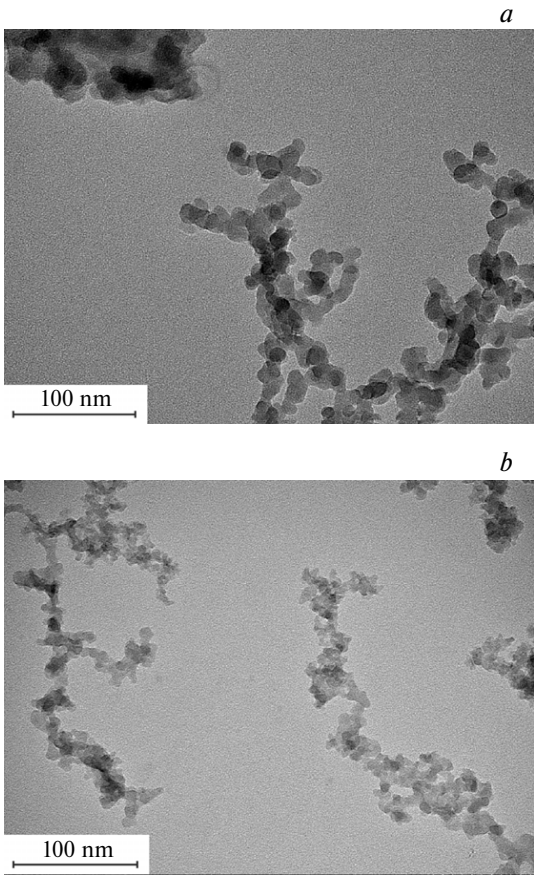

Fig. 3. TEM images of particles formed during surface modification of SiO_2 with 3-aminopropyltriethoxysilane (**I**) (*a*) and 1,3-propanesultone (**II**) (*b*).

corresponding powders in water, were mixed and, as a consequence, particles **III** were formed.

The second approach (Scheme 2) consisted in mixing the solutions of particles formed just after the *in situ* synthesis and thus particles **IV** were formed. Some of the self-assembling hybrid associates produced in the second method were heated at 220 °C and yielded mixed particles **V**.

DLS data and polydispersity index for self-assembled hybrid associates consisting of positively charged aminated ($\zeta = 11$ mV) and negatively charged sulfonated ($\zeta = -43$ mV) SiO_2 nanoparticles provided an evidence to that systems **III** (polydispersity index of 0.44, mean particle diameter of 300 nm) and **IV** (polydispersity index of 0.32, mean particle diameter of 311 nm) were characterized by polymodal distribution of composing associates; while homogeneous distribution of associates was observed in the system **V** (polydispersity index of 0.2, mean particle diameter of 406 nm). It is noteworsy that when heated, the polymodal particle-size distribution in the system **III** transformed into stable monomodel distribution with a polydispersity index of 0.1 and particle diameter of 181 nm. The observed effect is likely due to the formation of ion pairs $[NH_3^+] + [SO_3^-]$ (Table 1).

The surface charge of the hybrid associates depends on the amount of functional groups on the surface. Thus, for the first synthesis approach, in which mixed particles **III** were formed, an amount of sulfonate groups on the surface of particles **II** (0.036—0.046 mmol m^{-2}) applied for the synthesis is greater than an amount of amino groups on the surface of particles **I** (0.020—0.026 mmol m^{-2}). Therefore, at mixing these particles, the surface charge of

Scheme 2

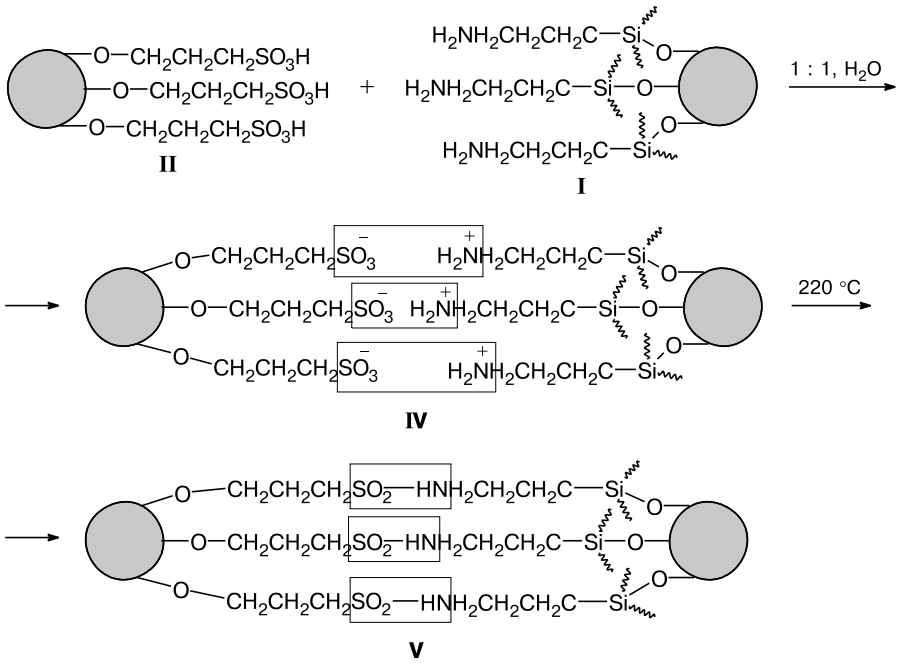

Table 1. Dynamic light scattering characteristics (diameter of associates *d*, polydispersity index PDI, ζ-potential) of modified (**I** and **II**) and mixed particles (**III**, **IV**, **V**), as well as pH values of the solutions

Particle	Solvent, conditions	*d*/nm	PDI	ζ	pH
I	H_2O	290±31	0.24±0.03	11.3±1.5	6.6
II	H_2O	201±17	0.23±0.04	−43.1±1.4	4.2
III	H_2O	300±115	0.44±0.03	−25.7±1.4	6.1
	H_2O, after heating	270±24	0.28±0.03	−31.6±2.9	5.6
	H_2O, after 24 h	181±16	0.10±0.08	−21.4±1.3	6.0
IV	H_2O	311±20	0.32±0.02	12.4±0.8	5.4
V	H_2O	406±38	0.20±0.02	4.7±0.4	4.5

the formed hybrid associates is negative (ζ = −26 mV). The surface of self-assembled mixed particles **IV**, produced by the second method, is positively charged (ζ = 12 mV) accounting that an amount of surface modifiers was equal. After heat treatment, the surface of the latter particles was nearly uncharged (ζ = 5 mV), which is probably due to the formation of covalent bonds between amino groups and sulfonate groups of the modified silica particles (**V**, see Scheme 2). Thus, the surface charge of self-assembled hybrid associates formed by aminated and sulfonated silica particles in water depends on the conditions for the particle synthesis.

Adsorption of macromolecules on the surface of hybrid silica nanoparticles. Implementation of targeted drug delivery systems which enable direct transportation of the required doses of active components is one of the challenges that modern pharmacology faces. Materials which are able to both selectively and reversibly bound with biologically important macromolecules are considered as promising therapeutic and diagnostic agents. In addition, those which can recognize/immobilize, for example, DNA molecules or various types of proteins, are of interest as carriers of biologically important macromolecules into the body cells. Hybrid silica-based organic-inorganic compositions may be attributed to these promising materials capable of recognizing/extracting biologically important compounds.

In the present work, we studied interaction of silica particles with biologically important macromolecules using aminated and sulfonated SiO_2 nanoparticles as well as mixed particles based on them as an example. The ability of charged SiO_2 particles to anchor DNA and proteins was estimated using UV spectroscopy and DLS

Silica particles containing primary amino groups as terminal functional groups, as well as mixed particles characterized by a total positive charge, **IV** and **V**, can anchor high molecular weight anionic substrates, such as DNA, mainly by electrostatic and hydrogen interactions and hence various associates are formed. In the electronic absorption spectra of calf thymus DNA, in the presence of various types of positively charged nanoparticles (**I**, **IV**, **V**) at pH 7.4 (in a buffer of 10 m*M* Tris-HCl, 10 m*M* of NaCl), hypochromic effects were observed in the region of 270 nm for all types of particles. As an example, Fig. 4 shows the absorption spectra for the system **I**—DNA.

The method for determining the efficiency of extraction of the adsorbate from solution *R* is described in the Experimental. *R* values (%) characterizing the adsorption of calf thymus DNA by modified silica particles **I** and mixed particles **IV** and **V** are present below.

Particle	*R* (%)
I	10.32±1.01
IV	6.20±0.90
V	28.14±1.50

One can see that among the studied samples, particles **V**, which were subjected to heat treatment appeared to be the most efficient in DNA extraction.

It was established that the efficiency of adsorption of model DNA (high molecular calf thymus DNA) in the series of modified silica particles studied increases with increasing ζ-potential: for "buffer" mixed submicron

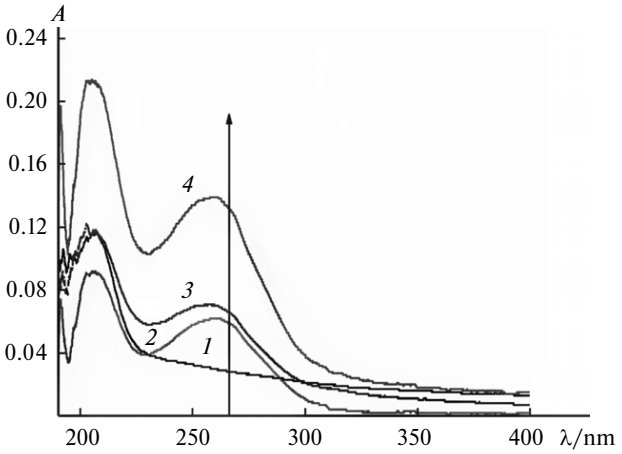

Fig. 4. Electron absorption spectra of particles **I** ($1.7 \cdot 10^{-5}$ g mL^{-1}) (*1*), calf thym us DNA in the absence (*2*) and in the presence of particles **I** (*3*), additive spectrum (pH 7.4, 10 m*M* Tris-HCl buffer, 10 m*M* NaCl) (*4*).

particles (4.7), aminated nanoparticles (11.3), and cross-linked submicron particles (12.4) it was 6, 10, and 28%, respectively.

In addition, the adsorption of lysozyme and bovine serum albumin (BSA) on the surface of negatively charged sulfonated silica particles **II** was studied. The efficiency of interaction of negatively charged particles **II** with proteins are present below.

Protein	*R* (%)
BSA (pH 6.86, phosphate buffer)	24.26±1.60
BSA (pH 9.18, phosphate buffer)	9.89±0.94
Lysozyme (pH 6.86, phosphate buffer)	37.09±1.10
Lysozyme (pH 7.40, Tris-HCl)	8.95±0.50
Lysozyme (pH 9.18, phosphate buffer)	27.17±1.15

The isoelectric point p*I* of lysozyme is 11.1 and, at given pH (6.86, 7.40, and 9.18), the protein was positively charged. Consequently, the strength of interaction of negatively charged sulfonated silica particles and positively charged lysozyme was governed by electrostatic interactions. The efficiency of adsorption of lysozyme was lower in Tris-HCl (pH 7.4), and higher in phosphate buffer solution at pH 6.86. The isoelectric point p*I* of BSA was 4.0 and at pH > p*I* its surface was charged negatively. Despite this, an efficient extraction of negatively charged BSA by negatively charged sulfonated particles was observed at given pH. As evident from the presented data, the interaction of the studied model proteins (BSA and lysozyme) with the synthesized silica nanoparticles **II** modified by sulfonate groups increased as pH of the medium decreased.

As it follows from the absorption spectra of sulfonated particles **II** with albumin at various amounts of BSA (pH 6.86, 10 m*M* phosphate buffer, 10 m*M* NaCl), an increase in concentration of BSA (from $1.6 \cdot 10^{-5}$ mol L^{-1}) in mixtures with sulfonated particles ($2.0 \cdot 10^{-5}$ g mL^{-1}) resulted in a hyperchromic effect in the region of 300—450 nm (Fig. 5). The linearization of the UV titration curves at a wavelength of 290 nm made it possible to determine the association constant: 10^5 (see Fig. 5).

Formation of associates in the system BSA—sulfonated silica particles was shown by DLS. It was found that albumin solution in phosphate buffer was characterized by high polydispersity (PDI = 0.59±0.02). When protein was mixed with the particles, the polydispersity nearly twice decreased (PDI = 0.35±0.05) due to formation of nanosized associates with an average hydrodynamic diameter of 187 nm. The formation of associates between BSA and sulfonated silica particles was observed under conditions when the macromolecule and nanoparticles had the same charge. This is probably due to the fact that sulfonated silica particles can interact with specific fragments of the BSA globule, the charge of which was different from the total charge of the protein.

Thus, it is the first time when SiO_2 nanoparticles (12 nm) were modified by 1,3-propanesulton and 3-aminopropyl triethoxysilane and nanoparticles containing amino and sulfonate groups were synthesized, the structure, composition, and identity of which were testified by ^{1}H NMR, IR and UV spectroscopy, TG/DSC, DLS. By varying methods for producing silica nanoparticles modified by amino and sulfonate groups, as well as conditions for their interaction (solvent, temperature), three protocols for the synthesis of different "buffer" mixed submicron particles with corresponding ζ-potentials ((–21.4±1.3, 4.7±0.4, 12.4±0.8) were developed. It was established that in the series of modified silica particles studied, the efficiency of extraction of model DNA (high molecular calf thymus DNA) increased with increasing ζ-potential. The efficiency was 6, 10, and 28 % for the "buffer" mixed submicron particles (4.7), aminated nanoparticles (11.3), and cross-linked submicron particles (12.4), respectively. It is shown that the interaction of the studied model pro-

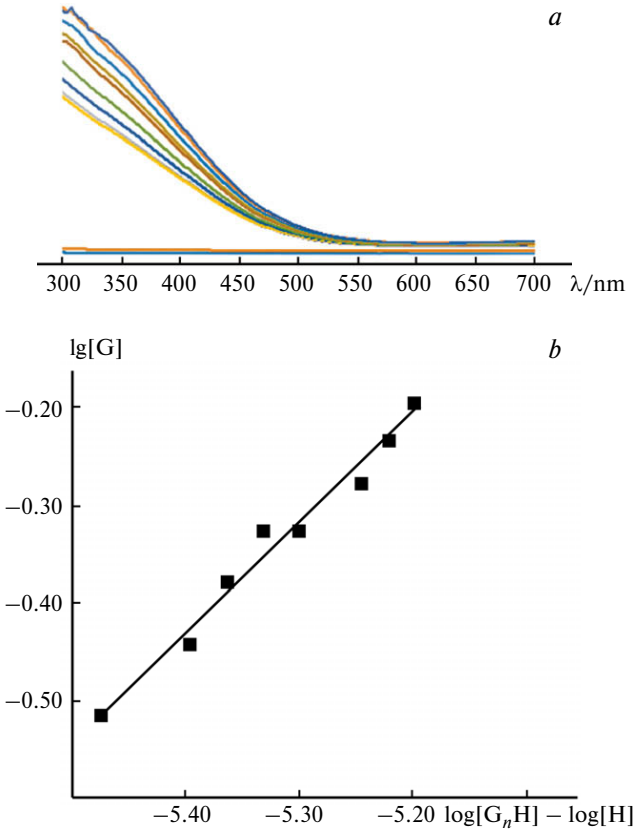

Fig. 5. (*a*) Absorption spectra of bovine serum albumin (pH 6.86, 10 m*M* phosphate buffer, 10 m*M* NaCl) in the absence of sulfonated particles **II** (yellow line) and at increased concentration of albumine (from $1.6 \cdot 10^{-5}$ mol L^{-1}), bottom orange line: absorbtion spectrum of nanoparticles **II** ($2.0 \cdot 10^{-5}$ g mL^{-1}); (*b*) dependency of log[G_nH] – log[H] from log[G], where log[G_nH] is the concentration of particles **II** and BSA, log[H] is the concentration of sulfonated particles **II**, log[G] is the BSA concentration; $y = 1.11x + 5.58$ ($R^2 = 0.98$).
Note. Fugure 5 is available in full color on the web page of the journal (http://www.link.springer.com/journal/11172).

teins (BSA and lysozyme) with synthesized silica modified by sulfonate groups increased as pH of the medium decreased.

This work was financially supported by the Russian Science Foundation (Project No. 18-73-10094).

References

1. R. K. Sharma, S. Sharma, S. Dutta, R. Zboril, B. D. Gawande, *Green Chem.*, 2015, **17**, 3207.
2. R. V. Ziatdinova, N. A. Losev, I. S. Terent´ev, A. V. Gerasimov, L. S. Yakimova, V. G. Evtugyn, I. I. Stoikov, *Russ. J. Gen. Chem.*, 2017, **87**, 1969.
3. L. S. Yakimova, O. A. Mostovaya, D. A. Bizyaev, A. A. Bukharaev, I. S. Antipin, A. I. Konovalov, I. Zharov, I. I. Stoikov, *Silicon*, 2011, **3**, 5.
4. I. I. Stoikov, A. A. Vavilova, R. D. Badaeva, V. V. Gorbachuk, V. G. Evtugyn, R. R. Sitdikov, L. S. Yakimova, I. Zharov, *J. Nanopart. Res.*, 2013, **15**, 1617.
5. G. V. Lisichkin, A. Yu. Fadeev, A. A. Serdan, P. N. Nesterenko, P. G. Mingalev, D. B. Furman, *Khimiya privitykh poverkhostnykh soedinenii* [*Chemistry of Anchored Surface Compounds*], Fizmatlit, Moscow, 2003, 592 pp. (in Russian).
6. A. A. Vertegel, R. W. Siegel, J. S. Dordick, *Langmuir*, 2004, **20**, 6800.
7. L. S. Yakimova, R. V. Ziatdinova, V. G. Evtugyn, I. Kh. Rizvanov, I. I. Stoikov, *Russ. Chem. Bull.*, 2016, **65**, 1053.
8. V. A. Burilov, A. T. Nurmukhametova, R. N. Belov, D. A. Mironova, V. V. Vorob´ev, Yu. N. Osin, I. S. Antipin, *Russ. Chem. Bull.*, 2018, **67**, 461.
9. A. L. Khan, C. Klaysom, A. Gahlaut, X. Li, I. F. Vankelecom, *J. Mater. Chem.*, 2012, **22**, 20057.
10. V. A. Burilov, A. T. Latypova, R. A. Safiullin, I. S. Antipin, *Russ. J. Gen. Chem.*, 2016, **86**, 661.
11. B. Bhushan, *Springer Handbook of Nanotechnology*, Springer-Verlag, GmbH, Germany, 2017, 1704 pp.
12. L. Zhao, Y. Zhao, Y. Han, *Langmuir*, 2010, **26**, 11784.
13. S. Xu, S. Hartvickson, J. X. Zhao, *J. Colloid Interface Sci.*, 2012, **134**, 15790.
14. A. Milogroom, M. Intrator, K. Madhavan, L. Mazzaro, R. Shandas, B. Liu, D. Park, *Colloids and Surfaces B: Biointerfaces*, 2014,**116**, 652.
15. S. H. Wu, Y. S. Lin, Y. Hung, Y. H. Chou, Y. H. Hsu, C. Chang, C.Y. Mou, *Chem Bio Chem*, 2008, **9**, 53.
16. J.E. Smith, L. Wang, W. Tan, *Trends Anal. Chem.*, 2006, **25**, 848.
17. Q. Mu, G. Jiang, L. Chen, H. Zhou, D. Fourches, A. Tropsha, B. Yan, *Chem. Rev.*, 2014, **114**, 7740.
18. P. Aggarwal, J. B. Hall, C. B. McLeland, M. A. Dobrovolskaia, S. E. McNeil, *Adv. Drug Delivery Rev.*, 2009, **61**, 428.
19. Z. G. Estephan, J. A. Jaber, J. B. Schlenoff, *Langmuir*, 2010, **26**, 16884.
20. K. D. Hartlen, A. P. T. Athanasopoulos, V. Kitaev, *Langmuir*, 2008, **24**, 1714.

Received November 20, 2018;
in revised form December 20, 2018;
accepted December 26, 2018